



Hybrid Nanocarbon Materials for Magnetic Resonance and Fluorescent Imaging: A Mini Review

Rui-Lin Liu^{1,2,*} and Jia-Xuan Hou¹

¹School of Pharmacy, Xi'an Jiaotong University, Xi'an 710061, PR China

²Department of Bioengineering, University of Texas at Arlington, Arlington, TX 76010, USA

Article info

Received 13 July 2017

Revised 10 December 2017

Published 01 January 2018

*Corresponding author: Rui-Lin Liu, School of Pharmacy, Xi'an Jiaotong University, Xi'an 710061, PR China;

E-mail: lrjtu1987@xjtu.edu.cn

Abstract

Carbon nanomaterials have gained significant momentum as promising candidate materials for biomedical applications due to their unique structure and properties. Carbon-based nanohybrids can be used as magnetic and fluorescent imaging contrast agent agents when it was functionalized by magnetic and fluorescent components. This mini-review summarizes the ultramodern applications and developments of hybrid carbon materials and addresses the future perspectives of carbon-based magnetic and fluorescent nanohybrids in the biomedical field.

Keywords: Carbon-based materials; Magnetic/fluorescent nanohybrids; Multi-modal imaging; Magnetic resonance; Fluorescent imaging.

Introduction

Multifunctional nanoparticles (MNPs) have drawn a lot of attention in recent years [1]. Various precursors have been used as substrates to fabricate multifunctional nanohybrids [2,5]. Among them, carbon-based substrates have been proven to have excellent potential with biocompatibility, large specific surface area, non-specific binding sites and easy surface modifications [6-9]. In particular, magnetic or fluorescent components in carbon-based nanohybrids can image the tissues for cancer diagnosis due to their characteristics of non-ionization, high spatial resolution, and deep tissue penetration for magnetic resonance imaging (MRI) or single-cell sensitivity and subcellular resolution for fluorescence optical imaging (FOI). But MRI alone has the disadvantages of poor sensitivity and FOI alone possesses bad spatial resolution and tissue penetration in clinical applications [10]. It's desirable to design new imaging agents that can combine more imaging modalities to address issues such as resolution, sensitivity, and tissue penetration [11-18].

In the mini review, we try to shortly review the recent developments and applications of carbon-based

magnetic and fluorescent nanohybrids as multi-modal imaging agents.

Multi-Modal Imaging

Early detection of tumor tissues in vivo by medical imaging is crucial in the fight against cancer. So far, a variety of imaging technologies have been developed and used in clinical medicine, including MRI, FOI, X-ray computed tomography (CT) imaging, positron-emission tomography (PET) imaging, and ultrasound imaging. Each imaging method has their advantages and disadvantages. MRI has exceptional spatial resolution but lacks sensitivity. FOI is relatively economical and very sensitive but cannot penetrate deep into all tissues in the body. CT and ultrasound imaging possesses high spatial resolution but low sensitivity. PET is relatively sensitive yet provides no structural information. Multi-modal imaging through synergistically combining two or more imaging modalities into a single one offers possibilities to address multiple issues such as resolution, sensitivity, and tissue penetration, because multimodality techniques have complementary and cross validation abilities [19,20]. For example, preclinical photoacoustic (PA) imaging is a hybrid

modality, combining the high contrast and spectroscopic-based specificity of optical imaging with the high spatial resolution of ultrasound imaging. PA imaging offers greater specificity than conventional ultrasound imaging with the ability to detect haemoglobin, lipids, water and other light-absorbing chromophores, but with greater penetration depth than purely optical imaging modalities that rely on ballistic photons [21,22]. Herein, we attach immense importance to multimodal imaging from the combination of MRI with FOI. The integration of magnetic and fluorescent components into the carbon-based hybrid NPs can provide not only the MRI contrast, but also the confocal, two-photon and NIR fluorescence imaging contrast [23-26].

Magnetic Resonance Imaging

MRI is a non-invasive imaging modality for determining the presence, location and size of a tumor in clinical tests, based on the alignment/spins of hydrogen nucleus (proton) in an applied magnetic field [27]. Upon application of a transverse radiofrequency pulse, these protons are perturbed from the magnetic field. The subsequent process through which these protons return to their original state is referred to as the relaxation phenomenon. Two independent processes, longitudinal relaxation (T_1 -recovery) and transverse relaxation (T_2 -decay), can be monitored to generate an MR image.

Carbon-based hybrid NPs containing superparamagnetic or ferromagnetic or paramagnetic components are typically used to act as T_2 or T_1 phase contrast agents due to their negative and positive contrast enhancement using T_2 and T_1 -weighted pulse sequences, respectively. Wang et al. developed a type of multifunctional hybrid NPs (~100 nm) that combine fluorescent carbon dots (CDs) and magnetic Fe_3O_4 nanocrystals into a porous carbon matrix [23]. The resultant Fe_3O_4 @C-CDs hybrid NPs demonstrated a superparamagnetic behaviour with good magnetic responsive properties ($M_s=32.5 \text{ emu g}^{-1}$) and MRI ability ($r^2=674.4 \text{ mM}^{-1}\text{s}^{-1}$). As shown in **Figure 1**, Fe_3O_4 @C-CDs hybrid NPs with surface carboxyl/hydroxyl groups sufficiently disperse in aqueous solutions.

When the anisotropic field-induced magnetic dipolar interaction of Fe_3O_4 @C-CDs hybrid NPs was stronger than the Brownian motion and electrostatic repulsion in solution, the Fe_3O_4 @C-CDs hybrid NPs tended to assemble in a head-to-tail configuration, leading to the formation of a one-dimensional (1D) linear nanochain structure under an external magnetic field [28-32].

Interestingly, the dispersed 0D building block NPs exert lower MRI contrasting ability ($r^2=960.9 \text{ mM}^{-1}\text{s}^{-1}$) than the 1D nanochains assembled from the nearly monodisperse Fe_3O_4 @C-CDs hybrid NPs.[26] The increased magnetization and local magnetic field strength of the assembled Fe_3O_4 @C-CDs hybrid NP chains influenced surrounding protons to transversely relax faster and resulted in such an enhancement in the T_2 -weighted MRI contrasting ability of the 1D structured NP chains [33]. Yang et al. proved that NIR fluorescent CdTe quantum dots (QDs) and superparamagnetic iron oxide (SPIO) NPs were coupled onto the surface of carbon nanotubes as multimodal cellular imaging agents were used for detecting human embryonic kidney (HEK) 293T cells [34]. Compared with the SPIO-CdTe bicomponent NPs, it exerted higher intracellular labelling efficiency because of the enhanced penetration ability of carbon nanotubes into cells.

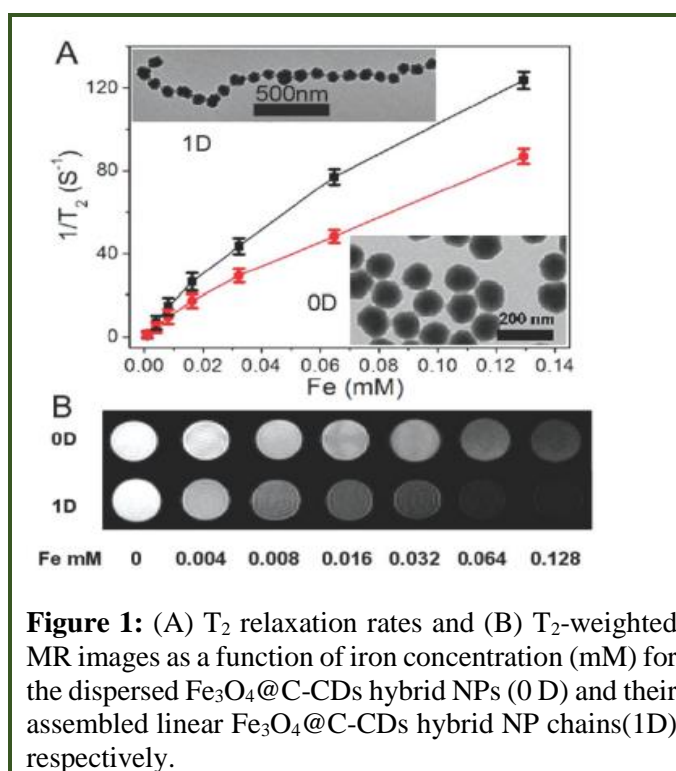


Figure 1: (A) T_2 relaxation rates and (B) T_2 -weighted MR images as a function of iron concentration (mM) for the dispersed Fe_3O_4 @C-CDs hybrid NPs (0D) and their assembled linear Fe_3O_4 @C-CDs hybrid NP chains(1D) respectively.

Fluorescence Imaging

Fluorescence intracellular imaging is a suitable technology to sense physical and chemical changes in the body because the fluorescence signal variation is sensitive, selective, rich in contrast, and versatile. Meanwhile, the intracellular probing of these events can contribute to the explanation of intricate biological processes and the development of novel diagnoses. Many fluorescent probes have been used as optical signals for fluorescence intracellular imaging. The

incorporation of different fluorophores into nanostructured magnetic-carbon hybrids has led to the successful combination of MRI modality with confocal fluorescence imaging, or two-photon fluorescence imaging, or NIR fluorescence imaging modality [35-42].

Confocal Fluorescence Imaging

The confocal fluorescence imaging technique is the use of a range of distinct excitation wavelengths in the UV-visible light range. The excitation wavelengths is shorter than the detection wavelengths for the emissions. Chen and co-workers deposited Ag nanocrystals onto the surface of Fe₃O₄@C nanospheres and the as-made composite was used for both MRI and fluorescence imaging [43]. They also developed a monodisperse yolk-type Au@Fe₃O₄@C nanospheres as dual-probes for both MRI confocal fluorescence imaging [44].

Recently, CDs, a type of fluorescent carbon nanoparticles with a size below 10 nm, have received much attention because of their excellent optical properties including excitation-wavelength tunable emission and upconverted photoluminescence (PL). Compared with noble metal NPs, CDs demonstrate lower toxicity and better biocompatibility [45,46]. Particularly these CDs have not only bright nonblinking PL with excellent photo-stability but also photothermal conversion ability under NIR irradiation [47,48]. For example, Jiang et al. fabricated a novel magnetic fluorescent carbon nanohybrid (SPIO@CQDs) via the layer-by-layer assembly of SPIO NPs with carbon QDs, which demonstrated the successful bimodal cell imaging ability for both MRI and multicolour confocal fluorescence imaging [49]. As shown in **Figure 2**, SPIO@CQDs hybrid NPs can enter liver L02 cells and illuminate them brightly under laser excitation with wavelengths of 405 nm, 488 nm and 514 nm after a 6 h incubation, respectively [49].

Two-Photon Fluorescence Imaging

The two-photon fluorescence imaging technique uses red-shifted light (e.g. NIR range) for excitation. For each excitation, two photons of NIR light are absorbed. The multiphoton absorption strongly suppresses the background signal. Furthermore, using NIR light minimizes scattering in the tissue. Both effects lead to an increased penetration depth. Therefore, two-photon fluorescence imaging has attracted much attention because of its potential applications in direct observation of cellular structure and biological process with the advantages of deep penetration in biological tissues, low photobleaching and weak auto-

fluorescence [50]. Combining up-conversion fluorescent nanocrystals into carbon-based nanostructures can help us realize a new multifunctional imaging probe including the two-photon fluorescence imaging ability. It has been demonstrated by the integration of noble metal (Ag and Au) nanocrystals with the magnetic-carbon composite NPs through the excitation by femtosecond infrared laser of 720 nm and detection wavelength range of 408-464 nm [43,44].

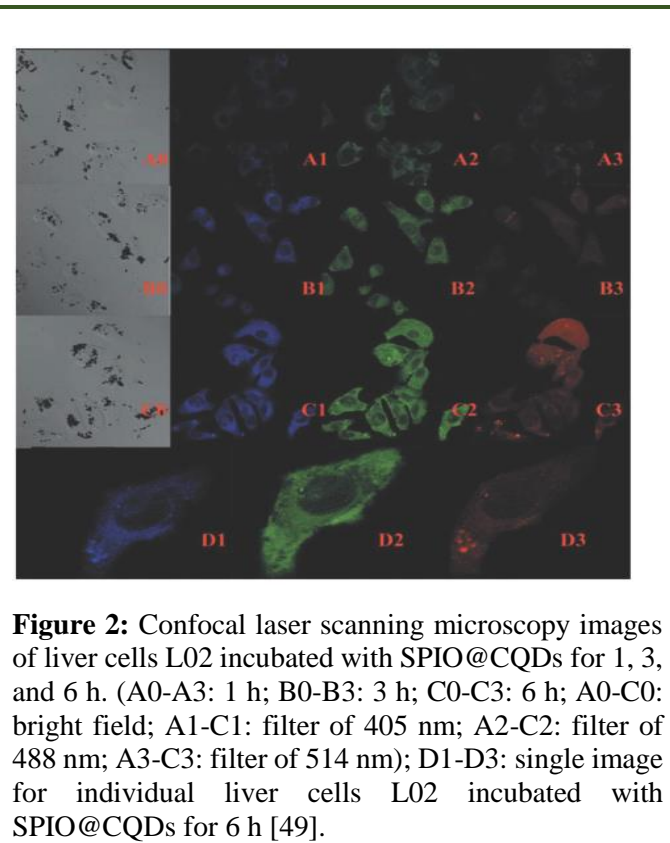


Figure 2: Confocal laser scanning microscopy images of liver cells L02 incubated with SPIO@CQDs for 1, 3, and 6 h. (A0-A3: 1 h; B0-B3: 3 h; C0-C3: 6 h; A0-C0: bright field; A1-C1: filter of 405 nm; A2-C2: filter of 488 nm; A3-C3: filter of 514 nm); D1-D3: single image for individual liver cells L02 incubated with SPIO@CQDs for 6 h [49].

Near-Infrared Fluorescence (NIRF) Imaging

The NIRF imaging technique uses excitation wavelengths in the NIR range and detects the emitted fluorescence above the excitation wavelengths. So NIRF imaging has better signal to-background separation, lower energy absorption and deeper penetration for human tissues [51,52]. NIR light can pass across several cm of heterogeneous living tissues because tissue auto-fluorescence and light absorption in the NIR range (650-900 nm) are low so that optical markers in the NIR wavelength range are of particular interest for *in vivo* imaging [53,53].

Conclusion

This mini-review summarizes the recent developments of carbon-based nanoscale systems for applications in the biomedical area. Various carbon-based multifunctional hybrid nanocarriers have been

developed for multi-modal imaging. Although there are the significant advances in the development of NPs, the clinical use of multifunctional hybrid nanocarriers is hindered by the challenge in delivering a clinically efficacious amount of chemotherapeutics to targeted cells and the unacceptable levels of off-target toxicity. Meanwhile, nonspecific cell targeting, poor bio-distribution and lack of non-invasive imaging of multifunctional hybrid nanocarriers limit their applications in vivo. Thus, there is an urgent need to develop a clinically useful multifunctional carbon-based imaging system.

Conflict of Interest

None declared.

Funding

None declared.

References

1. Wang H, Di J, Sun Y, et al. Biocompatible PEG-Chitosan@carbon dots hybrid nanogels for two-photon fluorescence imaging, near-infrared light/pH dual-responsive drug carrier, and synergistic therapy. *Adv Funct Mater* 2015; 25: 5537–5547.
2. Wang D, Guo Z, Zhou J, et al. Novel $Mn_3[Co(CN)_6]_2@SiO_2@Ag$ core-shell nanocube: enhanced two-photon fluorescence and magnetic resonance dual-modal imaging-guided photothermal and chemo-therapy. *Small* 2015; 11: 5956–5967.
3. Wang H, Shen H, Cao G, et al. Multifunctional PEG encapsulated $Fe_3O_4@silver$ hybrid nanoparticles: antibacterial activity, cell imaging and combined photo-thermo/chemo-therapy. *J Mater Chem B* 2013; 1: 6225–6234.
4. Wang H, Li Y, Luo Z, et al. Synthesis of PEG-encapsulated superparamagnetic colloidal nanocrystals clusters. *Nano* 2010; 5: 333–339.
5. Cui Y, Li B, He H, et al. Metal-organic frameworks as platforms for functional materials. *Acc Chem Res* 2016; 49: 483–493.
6. Justin R, Tao K, Román S, et al. Photo-luminescent and superparamagnetic reduced graphene oxide-iron oxide quantum dots for dual-modality imaging, drug delivery and photothermal therapy. *Carbon* 2016; 97: 54–70.
7. Tuček J, Kemp KC, Kim KS, et al. Magnetic and fluorescent carbon-based nanohybrids for multi-modal imaging and magnetic field/NIR light responsive drug carriers. *ACS Nano* 2014; 8: 7571–7612.
8. Wei W, Qu X. Extraordinary physical properties of functionalized graphene. *Small* 2012; 8: 2138–2151.
9. Hong T, Lazarenko RM, Colvin DC, et al. Effect of competitive surface functionalization on dual-modality fluorescence and magnetic resonance imaging of single-walled carbon nanotubes. *J Phys Chem C* 2012; 116:16319–16324.
10. Selvan ST. Silica-coated quantum dots and magnetic nanoparticles for bioimaging applications. *Biointerphases* 2010; 5: FA110–FA115.
11. Huang Y, Hu L, Zhang T, et al. $Mn_3[Co(CN)_6]_2@SiO_2$ core-shell nanocubes: novel bimodal contrast agents for MRI and optical imaging. *Sci Rep* 2013; 3: 2647.
12. Wang G, Su X. The synthesis and bio-applications of magnetic and fluorescent bifunctional composite nanoparticles. *Analyst* 2011; 136: 1783–1798.
13. Chen O, Riedemann L, Etoc F, et al. Magneto-fluorescent core-shell super-nanoparticles. *Nat Commun* 2014; 5: 5093.
14. Zhou Q, Mu K, Jiang L, et al. Glioma-targeting micelles for optical/magnetic resonance dual-mode imaging. *Int J Nanomed* 2015; 10: 1805–1818.
15. Barrow M, Taylor A, Nieves DJ, et al. Tailoring the surface charge of dextran-based polymer coated SPIONs for modulated stem cell uptake and MRI contrast. *Biomater Sci* 2015; 3: 608–616.
16. Naha PC, Hecht E, Chorny M, et al. Dextran coated bismuth-iron oxide nanohybrid contrast agents for computed tomography and magnetic resonance imaging. *J Mater Chem B* 2014; 2: 8239–8248.
17. Sun X, Cai W, Chen X. Positron emission tomography imaging using radiolabeled inorganic nanomaterials. *Acc Chem Res* 2015; 48: 286–294.
18. Zhou T, Wu B, Xing D. Bio-modified Fe_3O_4 core/Au shell nanoparticles for targeting and multimodal imaging of cancer cells. *J Mater Chem* 2012; 22: 470–477.
19. Chen J, Zhang W, Zhang M, et al. Mn(II) mediated degradation of artemisinin based on $Fe_3O_4@MnSiO_3$ -FA nano-spheres for cancer therapy in vivo. *Nanoscale* 2015; 7: 12542-12551.
20. Chen J, Zhang W, Guo Z, et al. pH-responsive iron manganese silicate nanoparticles as T1-T2 dual-modal imaging probes for tumor diagnosis. *ACS Appl Mater Interfaces* 2015; 7: 5373–5383.
21. Xia J, Yao J, Wang LV. Photoacoustic tomography: principles and advances. *Electromagn Waves* 2014; 147: 1–22.
22. Beard P. Biomedical photoacoustic imaging. *Interface Focus* 2011; 1: 602–631.

23. Wang H, Shen J, Li Y, et al. Magnetic iron oxide–fluorescent carbon dots integrated nanoparticles for dual-modal imaging, near-infrared light-responsive drug carrier and photothermal therapy. *Biomater Sci* 2014; 2: 915–923.
24. Yang K, Hu L, Ma X, et al. Multimodal imaging guided photothermal therapy using functionalized graphene nanosheets anchored with magnetic nanoparticles. *Adv Mater* 2012; 24: 1868–1872.
25. Chen B, Zhang H, Zhai C, et al. Carbon nanotube-based magnetic-fluorescent nanohybrids as highly efficient contrast agents for multimodal cellular imaging. *J Mater Chem* 2010; 20: 9895–9902.
26. Wang H, Mararenko A, Cao G, et al. Multifunctional 1D magnetic and fluorescent nanoparticle chains for enhanced MRI, fluorescent cell imaging, and combined photothermal/chemotherapy. *ACS Appl Mater Interfaces* 2014; 6: 15309–15317.
27. Sun C, Lee JS, Zhang M. Magnetic nanoparticles in MR imaging and drug delivery. *Adv Drug Delivery Rev* 2008; 60: 1252–1265.
28. Wang H, Chen QW, Yu YF, et al. Assembly of superparamagnetic colloidal nanoparticles into field-responsive purple Bragg reflectors. *Dalton Trans* 2011; 40: 4810–4813.
29. Wang H, Chen QW, Sun LX, et al. Magnetic-field-induced formation of one-dimensional magnetite nanochains. *Langmuir* 2009; 25: 7135–7139.
30. Wang H, Yu Y, Sun Y, et al. Magnetic nanochains: a review. *Nano* 2011; 6: 1–17.
31. Hu H, Chen Q, Wang H, et al. Reusable photonic crystal with water as ink prepared by radical polymerization. *J Mater Chem* 2011; 21: 13062–13067.
32. Cheng K, Chen Q, Wu Z, et al. Colloids of superparamagnetic shell: synthesis and self-assembly into 3D colloidal crystals with anomalous optical properties. *Cryst Eng Comm* 2011; 13: 5394–5400.
33. Jaganathan H, Hugar DL, Ivanisevic A. Examining MRI contrast in three-dimensional cell culture phantoms with DNA-templated nanoparticle chains. *ACS Appl Mater Interfaces* 2011; 3: 1282–1288.
34. Chen B, Zhang H, Zhai C, et al. Carbon nanotube-based magnetic-fluorescent nanohybrids as highly efficient contrast agents for multimodal cellular imaging. *J Mater Chem* 2010; 20: 9895.
35. Bourlinos AB, Bakandritsos A, Kouloumpis A, et al. Gd(III)-doped carbon dots as a dual fluorescent-MRI probe. *J Mater Chem* 2012; 22: 23327.
36. Zhang M, Cao Y, Chong Y, et al. Graphene oxide based theragnostic platform for T1-weighted magnetic resonance imaging and drug delivery. *ACS Appl Mater Interfaces* 2013; 5: 13325–13332.
37. Romero-Aburto R, Narayanan TN, Nagaoka Y, et al. Fluorinated graphene oxide; a new multimodal material for biological applications. *Adv Mater* 2013; 25: 5632–5637.
38. Xu Y, Jia XH, Yin XB, et al. Carbon quantum dot stabilized gadolinium nanoprobe prepared via a one-pot hydrothermal approach for magnetic resonance and fluorescence dual-modality bioimaging. *Anal Chem* 2014; 86: 12122–12129.
39. Xu Y, Li YH, Wang Y, et al. ¹³C-engineered carbon quantum dots for *in vivo* magnetic resonance and fluorescence dual-response. *Analyst* 2014; 139:5134–5139.
40. Liao H, Wang Z, Chen S, et al. One-pot synthesis of gadolinium(III) doped carbon dots for fluorescence/magnetic resonance bimodal imaging. *RSC Adv* 2015; 5: 66575–66581.
41. Kanakia S, Toussaint JD, Chowdhury SM, et al. Physicochemical characterization of a novel graphene-based magnetic resonance imaging contrast agent. *Int J Nanomed* 2013; 8: 2821–2833.
42. Sitharaman B, Wilson LJ. International trial of the Edmonton protocol for islet transplantation. *Int J Nanomed* 2006; 1: 291–295.
43. Chen J, Guo Z, Wang HB, et al. Multifunctional Fe₃O₄@C@Ag hybrid nanoparticles as dual modal imaging probes and near-infrared light-responsive drug delivery platform. *Biomaterial* 2013; 34: 571–581.
44. Zhou YM, Wang HB, Gong M, et al. Yolk-type Au@Fe₃O₄@C nano-spheres for drug delivery, MRI and two-photon fluorescence imaging. *Dalton Trans* 2013; 42: 9906–9913.
45. Pan Y, Neuss S, Leifert A, et al. Size-dependent cytotoxicity of gold nanoparticles. *Small* 2007; 3: 1941–1949.
46. Yang ST, Wang X, Wang H, et al. Carbon dots as nontoxic and high-performance fluorescence imaging agents. *J Phys Chem C* 2009; 113: 18110–18114.
47. Wang H, Zhuang J, Velado D, et al. Near-infrared- and visible-light-enhanced metal-free catalytic degradation of organic pollutants over carbon-dot-based carbo-catalysts synthesized from biomass. *ACS Appl Mater Interfaces* 2015; 7: 27703–27712.
48. Yang ST, Cao L, Luo PG, et al. Carbon dots for optical imaging *in vivo*. *J Am Chem Soc* 2009; 131: 11308–11309.
49. Su X, Xu Y, Che Y, et al. A type of novel fluorescent magnetic carbon quantum dots for cells imaging and detection. *J Biomed Mater Res Part A* 2015; 103: 3956–3964.

50. Denk W, Strickler J Webb W et al. Two-photon laser scanning fluorescence microscopy. *Science* 1990; 248:73–76.
 51. Choi HS, Gibbs SL, Lee JH, et al. Targeted zwitterionic near-infrared fluorophores for improved optical imaging. *Nat Biotechnol* 2013; 31: 148–153.
 52. Mahmood U, Tung CH, Bogdanov AJ et al. Near-infrared optical imaging of protease activity for tumor detection. *Radiology* 1999; 213: 866–870.
 53. Park H, Crozier KB. Multispectral imaging with vertical silicon nanowires. *Sci Rep* 2013; 3: 2460.
 54. Choi Y, Kim S, Choi MH, et al. Highly biocompatible carbon nanodots for simultaneous bioimaging and targeted photodynamic therapy in vitro and in vivo. *Adv Funct Mater* 2014; 24: 5781–578.
-

This manuscript was peer-reviewed

Mode of Review: Single-blinded

Academic Editor: Dr. Imran Kazmi